Spin diffusion in low-dimensional copper-amino-acid complexes

1991 J. Phys.: Condens. Matter 3 1877

(http://iopscience.iop.org/0953-8984/3/12/018)

J. Phys.: Condens. Matter 3 (1991) 1877–1888. Printed in the UK

Spin diffusion in low-dimensional copper–amino acid complexes

P R Levstein†, H M Pastawski‡ and R Calvo§||

† Department of Chemistry, University of Massachusetts, Boston, MA 02125, USA
‡ Department of Physics, Massachusetts Institute of Technology, Cambridge, MA 02139, USA
§ Instituto de Desarrollo Tecnológico para la Industria Química, Güemes 3450, 3000 Santa Fe, Argentina

Received 24 April 1990, in final form 13 November 1990

Abstract. The magnetic dimensionality of paramagnets is responsible for the long time behaviour of their spin dynamics, where the decay of the correlation functions is governed by spin diffusion. To study this problem we have performed EPR measurements in single crystals of the copper complexes of L and DL racemic mixtures of the amino acids methionine and 2-aminobutyric acid. In all these systems the copper atoms are arranged in layers with Cu–Cu interlayer distances which are two or three times longer than those within the layers. In the DL compounds the copper atoms are located at inversion centres. There each copper atom is connected to four magnetically non-equivalent coppers via four identical pathways. In the L compounds this symmetry is broken and there are two distinct pairs of pathways connecting the four magnetically non-equivalent coppers. Consequently, each type of lattice (L or DL) has a different exchange network. That is, the DL compounds exhibit two-dimensional characteristics, while in the L compounds there is a preferred direction for the exchange coupling. This behaviour is manifested in the broader EPR linewidths of the L-type crystals as compared with those of the DL-types. To describe the changes in the spin correlation functions we introduce a model which allows for the quantum evolution of the spin system until many-body effects break down the quantum coherence. This time is of the order of $\hbar/\omega_e$, where ω_e is the exchange frequency. In the long-time regime, our model allows one to pass with continuity from correlation functions which are solutions of the diffusion equation in one dimension to those corresponding to two or three dimensions. The model explains successfully our experimental data and it may be applied to systems where the magnitude of the exchange coupling varies along different directions.

1. Copper–amino acid complexes: model systems for low-dimensional magnetic behaviour

In recent years great efforts have been made to correlate the sign and magnitude of exchange interactions between paramagnetic metal centres with their structural data [1]. The exchange interaction (J) is usually obtained from static susceptibility measurements performed at low temperatures. However, there are systems with magnitudes of J in the order of 0.1 K, where electron paramagnetic resonance (EPR) at

|| Also at: Facultad de Bioquímica y Ciencias Biológicas, Universidad Nacional del Litoral, Santa Fe, Argentina.

0953-8984/91/121877+12$03.50

room temperature is a well suited simpler technique. Consequently, theories relating experimental parameters such as the EPR linewidths with the exchange interaction constants are necessary.

The spin dynamics of a paramagnet are characterized by the latter's magnetic dimension. Its behaviour can be identified by EPR because spin diffusion, which is the mechanism that governs the spin dynamics at long times, has a strong dimensionality dependence, and produces characteristic changes in the linewidth and lineshape [2]. This dimensionality is generated by the network of exchange couplings and it does not necessarily coincide with that given by the crystallographic arrangement of the paramagnetic ions. This is particularly relevant in systems where the space symmetry is low. For example, in a structural 3D system, a two dimensional behaviour may appear if the exchange pathways between paramagnetic ions in a plane are more effective than those connecting ions in different planes. A further reduction in dimensionality would occur if there were a preferred direction for exchange within a layer. Thus, by analysing the dynamical behaviour of a spin system it is possible to draw conclusions about the effectiveness of the chemical paths for superexchange.

Copper–amino acid complexes ($Cu(AA)_2$) provide a convenient set of compounds to study changes of the low-dimensional magnetic behaviour around 2D. This is because they are structurally 2D and it is possible to crystallize several $Cu(AA)_2$ differing either in the interlayer exchange couplings or in the exchange network within a layer. In order to select the $Cu(AA)_2$ more suited to analyse the low-dimensional magnetic behaviour, we have taken into account the following facts.

(i) Correlations between the exchange coupling constant and the structural data in $Cu(AA)_2$ indicate that the length of the copper–apical oxygen bond of the carboxylate bridges is the major contributing factor to the strength of the superexchange interaction [3–5]. Besides, in several $Cu(DL\text{-}AA)_2$, the distances between one copper and its two apical oxygens are equal, while in the corresponding $Cu(L\text{-}AA)_2$ they differ by about 0.1 Å.

(ii) Magnetic susceptibility measurements at very low temperatures in the structurally 2D copper derivative of L-alanine, $Cu(L\text{-}ALA)_2$, indicate antiferromagnetic 1D chains [6].

Here we report single-crystal EPR measurements in $Cu(L\text{-}MET)_2$, $Cu(L\text{-}BUT)_2$, $Cu(DL\text{-}MET)_2$ and $Cu(DL\text{-}BUT)_2$, the copper derivatives of the amino acids L-methionine, L-2-aminobutyric acid, and of their racemic mixtures respectively. In all of them, the copper ions are arranged in layers. The L and DL complexes of the same amino acid have very similar crystal structures. However, in the DL compounds the coppers are at inversion centres, where the connections between one copper and its four copper neighbours are equal, while in the L compounds this symmetry is broken and there are two distinct pairs of identical pathways. These features suggested that the dimensionality of the exchange network might change from two in the DL compounds to a lower one in the L compounds because the latter have a preferential direction for exchange coupling. This change in the dimensionality produces large differences between the EPR linewidths of the L and DL compounds, which are readily observed in our experiments. In order to interpret our experimental results, we introduced a model for the high temperature spin correlation functions which describes the short and long-time regimes in terms of the microscopic parameters. This model is applied to cases where the exchange network is anisotropic, allowing us to handle systems where the behaviour of the spin diffusion ranges from 1D to 3D.

2. Magnetostructural correlations in copper–amino acid complexes

Crystallographic data of $Cu(DL\text{-}MET)_2$ [7], $Cu(L\text{-}MET)_2$ [8] and $Cu(DL\text{-}BUT)_2$ [9] have been reported. Since no previous data existed for $Cu(L\text{-}BUT)_2$ we performed its structural determination [10]. The relevant crystallographic information for the four compounds is displayed in table 1. Their structures consist of isolated sheets of Cu(II) ions with tetragonal N_2O_2 ligand sets, formed by trans coordination of two molecules of the corresponding amino acid. The apical Cu–O bonds result from interactions with carboxylate ions from neighbouring molecules. The two molecules of copper complex per unit cell ($Z = 2$) are related by a 180° rotation around the $\hat{b}$ axis, plus a translation. Then, there are two types of copper atoms chemically equivalent but magnetically non-equivalent which are called A and B in figure 1. The magnetically non-equivalent copper ions within a layer are connected by very weak N–H...O hydrogen bonds and by carboxylate bridges. In the $Cu(AA)_2$ studied here, as in others [3–4], the EPR resonances corresponding to magnetically non-equivalent species A and B are collapsed to a single line due to the exchange interaction. However, there is a contribution to the linewidth due to the difference between the gyromagnetic tensors of each type of copper. This contribution has well characterized angular and frequency dependences which allow its isolation. Then, it is possible to evaluate the exchange coupling constant between non-equivalent coppers $|J|$ using a model based in the Kubo–Tomita theory for magnetic resonance in coupled spin systems [11]. As this model does not consider low-dimensional effects, $|J|$ is evaluated with a systematic error which does not affect the main results if the interlayer distances are similar for the different systems under study, as will be shown later. Figure 2 displays the values of $|J|$ obtained using this method as a function of the shortest copper–apical oxygen bond length in three antiferromagnetic $Cu(L\text{-}AA)_2$: the copper derivatives of the amino acids L-phenylalanine, L-leucine and L-methionine. These $Cu(AA)_2$ have in common that they are magnetic layered systems with practically the same interlayer distances (around 15 Å). The strong correlation observed in figure 2 leads us to conclude that carboxylate bridges are the main paths for superexchange. On the other hand, no correlation was observed between the $|J|$ values obtained and the relevant parameters involved in H bonds. Therefore, we will neglect the contribution of hydrogen bonds to superexchange [5].

Table 1. Crystallographic data for the copper(II) salts of L-methionine [8], DL-methionine [7], L-2-aminobutyric acid [10] and DL-2-aminobutyric acid [9]. In the pair of complexes $Cu(L\text{-}BUT)_2$ and $Cu(DL\text{-}BUT)_2$ the layers of coppers are in the ab and bc planes respectively. Comparisons must be made between the $a(c)$ lattice parameter of $Cu(L\text{-}BUT)_2$ and the $c(a)$ of $Cu(DL\text{-}BUT)_2$.

	$Cu(L\text{-}MET)_2$	$Cu(DL\text{-}MET)_2$	$Cu(L\text{-}BUT)_2$	$Cu(DL\text{-}BUT)_2$
a (Å)	9.487(5)	9.482(5)	9.464(3)	11.138(6)
b (Å)	5.061(3)	5.018(4)	5.060(2)	5.066(1)
c (Å)	15.563(8)	16.035(13)	11.189(4)	9.487(6)
β (deg)	92.46(3)	93.78(4)	90.60(3)	92.15(6)
Space group	$P2_1$	$P2_1a$	$P2_1$	$P2_1c$
Z	2	2	2	2
Cu–O_{ap} (Å)	2.676		2.679	
	2.751	2.713	2.787	2.758

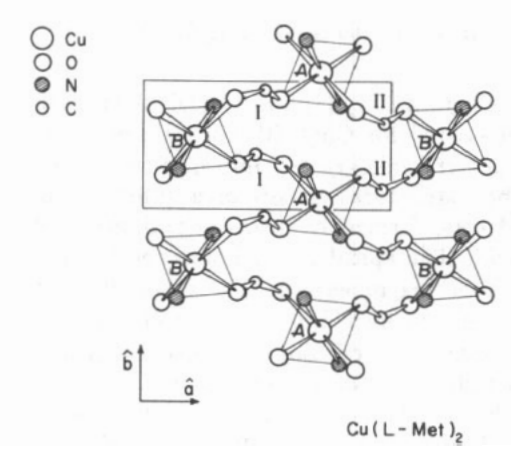

Figure 1. Orthogonal projection of a copper layer in a $Cu(L\text{-}AA)_2$ crystal lattice, showing the carboxylate sheet structure. The two types of carboxylate bridges are labelled as I and II.

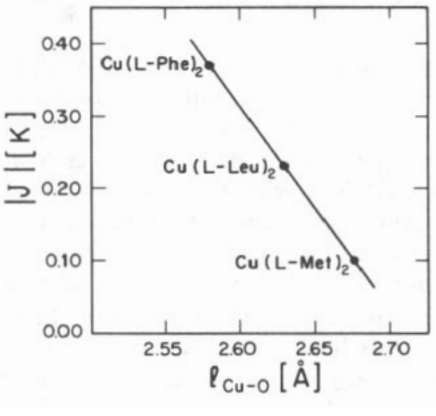

Figure 2. Variation of $|J|$ as a function of the shortest copper–apical oxygen bond length.

It is worthwhile to remark that, as can be seen in table 1, the DL compounds belong to the space groups $P2_1a$ and $P2_1c$ where the copper atoms are at inversion centres and the pathways between each copper and its four non-equivalent copper neighbours are equal. The L compounds, by contrast, belong to the space group $P2_1$ where the copper atoms are not at inversion centres and the paths between each copper and its four non-equivalent copper neighbours are only equal by pairs. This structural feature is of great importance in making the hypotheses concerning the exchange networks, and it is sketched in figure 3. The pairs of $Cu\text{–}O_{ap}$ bond lengths of the L compounds given in table 1 together with the data displayed in figure 2 allow us to estimate the anisotropy of the exchange network arising from the broken symmetry.

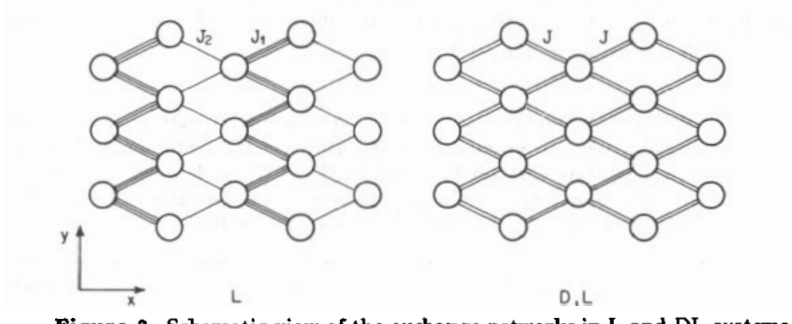

Figure 3. Schematic view of the exchange networks in L and DL systems.

3. Comparative analysis of the EPR data

Single-crystal EPR measurements of $Cu(L\text{-}BUT)_2$, $Cu(DL\text{-}BUT)_2$, $Cu(L\text{-}MET)_2$ and $Cu(DL\text{-}MET)_2$ were performed in the Q-band (34 GHz) and at room temperature.

The experimental details were described in [4]. To allow comparisons of the data, each sample was mounted on a sample holder, with the copper layers in the xy plane of an xyz reference system, and the $\hat{y}$ axis coincident with the crystallographic unique axis $\hat{b}$.

A single EPR line was observed in all cases for every orientation $\hat{h} = (\sin\theta\cos\phi, \sin\theta\sin\phi, \cos\theta)$ of the magnetic field $\boldsymbol{B}$. The squared gyromagnetic tensors were calculated from the position of the EPR line at each orientation. Figure 4 shows the experimental values for the squared gyromagnetic factor $g^2(\theta,\phi)$ obtained for Cu(DL-MET)$_2$. Experimental results for Cu(L-MET)$_2$ were reported in [4]. It is worthwhile to remark that the squared gyromagnetic tensors corresponding to Cu(L-MET)$_2$ and Cu(DL-MET)$_2$ are nearly equal, reflecting the very similar copper coordination and the same molecular axis orientation in the crystals. There is a small difference between the gyromagnetic tensors of Cu(L-BUT)$_2$ and Cu(DL-BUT)$_2$ due to the slightly different molecular orientation (approximately 3°). The angular variations of the peak-to-peak linewidths in both pairs of systems are displayed in figures 5 and 6. In all cases the linewidth data were least-square fitted to the function

$$\Delta B(\theta,\phi) = A_1\sin^2\theta\cos^2\phi + A_2\sin^2\theta\sin^2\phi + A_3\cos^2\theta + A_4 2\sin\theta\cos\phi\cos\theta + A_5(\sin^2\theta\cos\phi\sin\phi)^2 + A_6(\sin\phi\sin\theta\cos\theta)^2 + A_7\cos^4\theta. \quad (1)$$

The parameters A_i obtained from the fittings are given in table 2. The function in equation (1) involves the contributions to the broadening arising from the magnetic dipolar, hyperfine, residual Zeeman and antisymmetric exchange interactions [12]. Unfortunately, it is not possible to isolate the contribution of each of these interactions because of the strong correlations between the angular dependences of some of them (for example between the hyperfine and antisymmetric exchange interactions). Therefore, we will not attempt a detailed analysis of each contribution to the linewidth in this work, where we are mainly interested in understanding the striking difference between the EPR linewidths observed for the L and DL copper complexes of each amino acid. It is clear that the interactions mentioned above are not able to change the linewidth by themselves in the way shown in figures 5 and 6. The second moments of the magnetic dipolar, residual Zeeman, and hyperfine interactions do not change between L and DL systems because of the close similarity of the crystallographic arrangement of the copper ions and that of the molecular gyromagnetic and hyperfine tensors. In the case of the antisymmetric exchange, the contribution arising on the interaction between magnetically equivalent coppers vanishes in the DL systems. However, this contribution has a pure second-order angular variation, with an upper limit for its magnitude [13], which allows us to discard this contribution as the main source of the difference. As we will show in the next section, the experimental results indicate that the large changes of the linewidths between the L and DL complexes of the same amino acid are a manifestation of a change in the spin dynamics.

In order to obtain an experimental parameter accounting for the general features of the EPR linewidths, we performed the spherical average of the linewidth data. The ratio between these mean linewidths for the DL and the L complexes is $\widetilde{\Delta B}_{\mathrm{DL}}/\widetilde{\Delta B}_{\mathrm{L}} = 0.40 \pm 0.02$ for both pairs of systems.

4. Simple theory for spin diffusion

The EPR linewidth, $\Delta B(\theta,\phi)$, of an exchange-coupled spin system in the paramagnetic phase depends on the interactions producing local fields at each spin site and on

Table 2. Values of the parameters A_i (in gauss) obtained by fitting equation (1) to the experimental values of the linewidths measured at 34 GHz and 300 K, displayed in Figures 5 and 6. The uncertainties of these values were obtained from the dispersions of the fittings.

	$Cu(L\text{-}MET)_2$	$Cu(DL\text{-}MET)_2$	$Cu(L\text{-}BUT)_2$	$Cu(DL\text{-}BUT)_2$
A_1	82±2	48.6±0.6	101±1	38.4±0.5
A_2	69±3	68.9±0.6	83±1	52.3±0.6
A_3	91±14	33±3	11±8	26±3
A_4	44±2	3.0±0.5	42±1	3.9±0.5
A_5	262±15	56±3	45±8	55±3
A_6	598±18	90±4	197±10	87±4
A_7	179±15	140±3	206±8	104±3

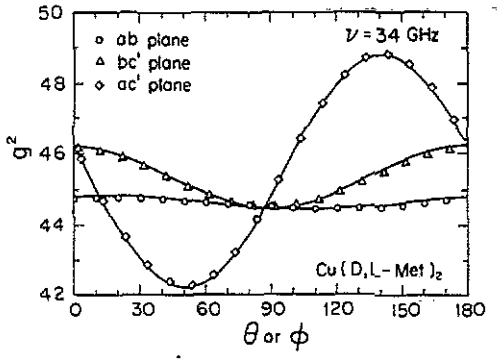

Figure 4. Angular variation of the squared gyromagnetic factor measured at 300 K and 34 GHz in three orthogonal planes of a $Cu(DL\text{-}MET)_2$ single crystal. The solid lines correspond to a least-squares fitting with a second order tensor.

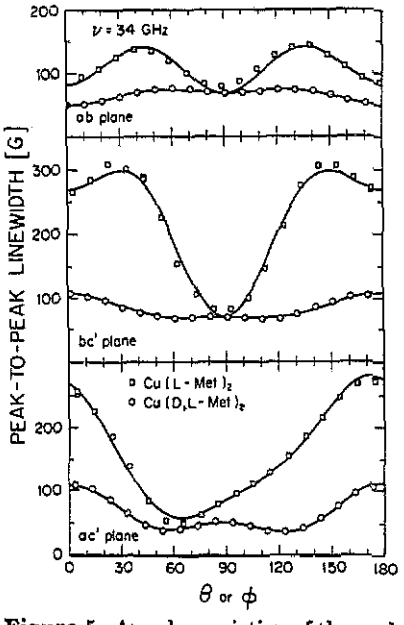

Figure 5. Angular variation of the peak-to-peak linewidths measured at 300 K and 34 GHz in the three principal planes of $Cu(DL\text{-}MET)_2$ and $Cu(L\text{-}MET)_2$ single crystals. The full curves were obtained from least-squares fits of the linewidth data in each system to equation (1).

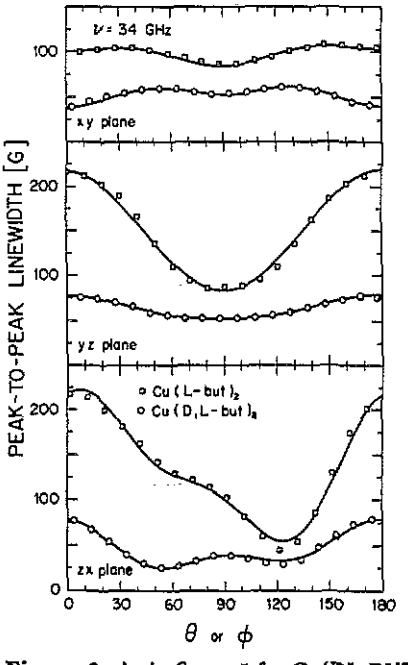

Figure 6. As in figure 5 for $Cu(DL\text{-}BUT)_2$ and $Cu(L\text{-}BUT)_2$.

the dynamics of these fields imposed by the exchange interaction. Following the perturbative approach introduced by Kubo and Tomita [11,12], and considering that the EPR data were taken at 34 GHz, the non-secular contributions [14] can be neglected. Then $\Delta B(\theta,\phi)$ can be expressed as:

$$\Delta B(\theta,\phi) = \frac{2}{\sqrt{3}\hbar^2}\int_0^\infty \frac{\langle[\mathcal{H}'_{\rm sec}(t),S^+][S^-,\mathcal{H}'_{\rm sec}]\rangle}{\langle S^+S^-\rangle}\,{\rm d}t. \tag{2}$$

The argument of the integral is the exchange modulated local field correlation function corresponding to $\mathcal{H}'_{\rm sec}$, the secular component of perturbative interactions $\mathcal{H}'$. In these systems [12], $\mathcal{H}'$ consists of the dipole–dipole, hyperfine and residual Zeeman interactions. The time dependence of $\mathcal{H}'_{\rm sec}(t)$ is produced by the exchange Hamiltonian,

$$\mathcal{H}'_{\rm sec}(t) = \exp({\rm i}\mathcal{H}_{\rm ex}t/\hbar)\mathcal{H}'_{\rm sec}\exp(-{\rm i}\mathcal{H}_{\rm ex}t/\hbar)$$

with

$$\mathcal{H}_{\rm ex} = \tfrac{1}{2}\sum_{i,j} J_{ij}\boldsymbol{S}_i\cdot\boldsymbol{S}_j. \tag{3}$$

For the present purpose $2N+1$ spins 1/2 are arranged on an orthorhombic lattice. Only the exchange constants $J_{ij} = J_\nu$ (ν=1, 2, 3) for the z_ν nearest neighbours in the ν direction are considered to be different from zero. The corresponding lattice parameters are a_ν.

In order to give an insight into the essential features governing the spin dynamics, we are going to treat interactions linear in electronic spin operators as the hyperfine interaction. In this case we obtain,

$$\langle[\mathcal{H}'_{\rm sec}(t),S^+][S^-,\mathcal{H}'_{\rm sec}]\rangle/\langle S^+S^-\rangle = M_2^{\rm sec}(\theta,\phi)\langle S_i^z(t)S_i^z\rangle/\langle S_i^zS_i^z\rangle \tag{4}$$

where $M_2^{\rm sec}(\theta,\phi)$ is the secular component of the second moment of the considered interaction and

$$S_i^z(t) = \exp({\rm i}\mathcal{H}_{\rm ex}t/\hbar)S_i^z\exp(-{\rm i}\mathcal{H}_{\rm ex}t/\hbar). \tag{5}$$

Then the EPR linewidth is proportional to the integral of the self-site spin correlation function:

$$\Delta B_1(\theta,\phi) = \frac{2}{\sqrt{3}\hbar^2}M_2^{\rm sec}(\theta,\phi)\int_0^\infty \frac{\langle S_i^z(t)S_i^z\rangle}{\langle S_i^zS_i^z\rangle}\,{\rm d}t \tag{6}$$

where the subscript 1 indicates contributions to $\Delta B(\theta,\phi)$ linear in spin operators. The evaluation of this self-site spin correlation function (or local magnetization) has been discussed by a number of authors [15] and it is not free of conceptual and mathematical difficulties. In 3D it leads to integro-differential equations which must be solved numerically [15a]. On the other hand, Richards [2] has shown that these results are not applicable to low-dimensional magnetic systems because they fail to describe the intermediate and long-time regimes, which determine the time integral of the correlation function. In the L-systems the relation between the exchange coupling constants in the different directions verifies approximately $J_1 \approx 4J_2 \approx 24J_3$. Here, the relation

between J_1 and J_2 was evaluated from the correlations displayed in figure 2, and the Cu–O_{ap} lengths given in table 1. The relation between the intralayer couplings (J_1 and J_2) and the interlayer one (J_3) was estimated using the magnetic susceptibility data taken on a single crystal of $Cu(L\text{-}ILE)_2$, the copper derivative of L-isoleucine [16]. Therefore, a simple description giving the diffusive time dependence in a complete range of exchange magnitudes is crucial.

In order to analyse the dynamics of the 2N+1 spins, it is convenient to separate the exchange Hamiltonian into two parts $\mathcal{H}_{ex} = \mathcal{H}_i + \mathcal{H}_{mb}$. We call $\mathcal{H}_i$ the part determining the quantum evolution of a single spin which is originally at site i in a lattice with all the other spins frozen in each of the $(2N!)/(N!)^2$ possible initial configurations. Each configuration generates an independent subspace of dimension N or lower, in which the $\mathcal{H}_i$ has an upper bound for the connectivity given by the number of nearest neighbours $z = z_1 + z_2 + z_3$. This one-body part governs the short-time evolution but it is unable to produce spin diffusion because of quantum interference, as proved by Anderson for spin dynamics [17a] and generalized in the context of quantum localization [17b,c]. In the 'many-body' part, $\mathcal{H}_{mb}$, we include all other configurations and matrix elements not included in $\mathcal{H}_i$. We will analyse how the phase breaking of the one-body quantum evolution manifests itself on the time dependence of the magnetization in the high temperature limit. The lowest order of the series expansion of equation (5) which contributes to the self-site spin correlation function, has contributions from $\mathcal{H}_i$ only and gives

$$m(t) = \frac{\langle S_i^z(t) S_i^z \rangle}{\langle S_i^z S_i^z \rangle} \approx 1 - \tfrac{1}{2}\langle z_1 \rangle \frac{J_1^2 t^2}{\hbar^2} - \tfrac{1}{2}\langle z_2 \rangle \frac{J_2^2 t^2}{\hbar^2} - \tfrac{1}{2}\langle z_3 \rangle \frac{J_3^2 t^2}{\hbar^2} \tag{7}$$

where $\langle z_\nu \rangle$ is the thermal average of the number of sites available for the exchange in the ν direction i.e. $\langle z_\nu \rangle = 1$ is the mean of 2(once), 1(twice) and 0(once). An essential point to observe is that in absence of $\mathcal{H}_{mb}$, this average involves individual evolutions in the range $[1, 2m(t) - 1]$, corresponding to the 2^z possible configurations of nearest neighbours. These individual evolutions are mixed by the $\mathcal{H}_{mb}$ terms which appear in the t^4 order. Therefore, for the time at which $m = 1/2$ there are individual magnetizations dispersed in the whole range (1,0) because of the 'many-body' effect. This is the phase-breaking time, which results in:

$$\tau_\phi = \hbar / \sqrt{(z_1 J_1^2 + z_2 J_2^2 + z_3 J_3^2)/2} = 1/\omega_e. \tag{8}$$

This time can be regarded as a characteristic clock's tick at which the modification of the frozen environment occurs (a phase breaking collision). Therefore, the one-body quantum probability must be evaluated [18] and a new one-body quantum evolution starts until a subsequent 'collision'. This process can be taken as a discrete-time random walk or as a continuous-time random walk with an exponential distribution of waiting time [19]. Both give a diffusive behaviour for the magnetization [20]. At the first 'collision', quantum and classical hopping probabilities must be identical,

$$\begin{aligned} m_{quant}(\tau_\phi) &\approx 1 - \tfrac{1}{2} J_1^2 \tau_\phi^2/\hbar^2 - \tfrac{1}{2} J_2^2 \tau_\phi^2/\hbar^2 - \tfrac{1}{2} J_3^2 \tau_\phi^2/\hbar^2 \\ &\equiv m_{clas}(\tau_\phi) = 1 - 2D_1 \tau_\phi/a_1^2 - 2D_2 \tau_\phi/a_2^2 - 2D_3 \tau_\phi/a_3^2 \end{aligned} \tag{9}$$

and from this identity we extract the spin diffusion constants:

$$D_\nu = a_\nu^2 J_\nu^2 \tau_\phi / 4\hbar^2. \tag{10}$$

Thus, the key for the irreversible decay of the local magnetization is that the time evolution of a single spin occurs in a fluctuating environment produced by its neighbouring spins, which change at the same rate. Because of the number of states involved, these play the role of a 'thermal bath' which determines the characteristic time τ_ϕ at which the quantum coherence of the single-particle description breaks down.

A convenient continuous-time description of $m(t)$ can be given as the weight over the unit cell of a density $C_1C_2C_3$, which behaves diffusively in each direction: $C_\nu(x_\nu,t) = (4\pi D_\nu t)^{-1/2}\exp(-x_\nu^2/4D_\nu t)$. This gives

$$m(t) = m_1(t)m_2(t)m_3(t) \tag{11}$$

with

$$m_\nu(t) = \int_{-a_\nu/2}^{a_\nu/2} C_\nu(x_\nu,t)\,\mathrm{d}x_\nu = \mathrm{erf}\left(\frac{a_\nu}{4\sqrt{D_\nu t}}\right).$$

This description of the local magnetization, although not very accurate for short times, avoids the short-time divergences and maintains a consistent normalization which allows the evaluation of other pair spin correlation functions $\langle S_j^z(t)S_i^z\rangle$.

In order to apply the present theory to our systems we must take into account that the interlayer exchange is very weak [16], ($J_3 \to 0$) and therefore, $m_3(t) \approx 1$ for the times of interest ($t < a_3^2/D_3$). Another consideration is that at every time of the random walk, the self correlations in the lattices of figure 3 are equal to those of a square lattice even when $J_1 \neq J_2$. Hence, the experimental situation corresponds to that analysed above.

To perform a microscopic evaluation of the asymmetry in the L compounds, we resort to the Anderson result for the superexchange constant. Thus, the antiferromagnetic contribution to J [17b] is $2|\tilde{V}|^2/U$. Here U is the Hubbard repulsion for two electrons in the same copper and $\tilde{V}$ is the nearest neighbour effective hopping parameter which sums up contributions from the different chemical paths [21]. In our systems the main contribution comes from the carboxylate bridges [5] and $\tilde{V}$ results proportional to $S_{\mathrm{Cu-O}} \sim \exp(-R/\lambda)$, the overlap between the copper $d_{x^2-y^2}$ and the apical-oxygen sp^2 orbitals; here R is the Cu-O_{ap} bond length and λ is the attenuation constant. The distance R is the only parameter which changes significantly from L to DL complexes. This variation ΔR produces, at first order, a variation of J,

$$\Delta J \approx -2J\Delta R/\lambda. \tag{12}$$

Therefore, we should expect that if the displacement of the apical oxygens in the L-systems (as compared to DL) conserves the arithmetic mean, as it is approximately the experimental situation (see table 1), the same should hold for the exchange constant J. Then, in an L system $J_1 = J + \Delta J$ and $J_2 = J - \Delta J$, where J is the exchange constant in the respective DL-system. Besides, using the magnetostructural correlations displayed in figure 2 , which fit to a value of $\lambda \approx a_0/3$ (a_0 is the Bohr radius), it can be estimated that $J_1 \approx 4J_2$. Hence, from equations (8)–(10), it results that $D_1/a_1^2 = 0.39\ J/\hbar$ and $D_2/a_2^2 = 0.024\ J/\hbar$, and in the corresponding DL-system $D_1/a_1^2 = D_2/a_2^2 = 0.18\ J/\hbar$. The time dependence of $\langle S_i^z(t)S_i^z\rangle/\langle S_i^z S_i^z\rangle$ obtained with these parameters is shown in figure 8. The faster quantum decay in the L-system implies an earlier start of the diffusive behaviour, leading to a slower decay and a

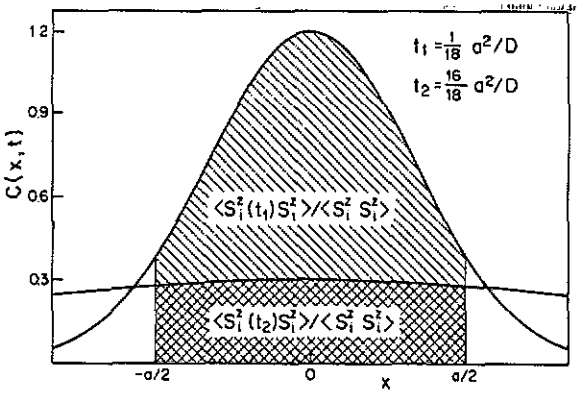

Figure 7. Time evolution of the spin density around site i. At $t \ll a^2/D$ the spin excitation remains mainly in the original site.

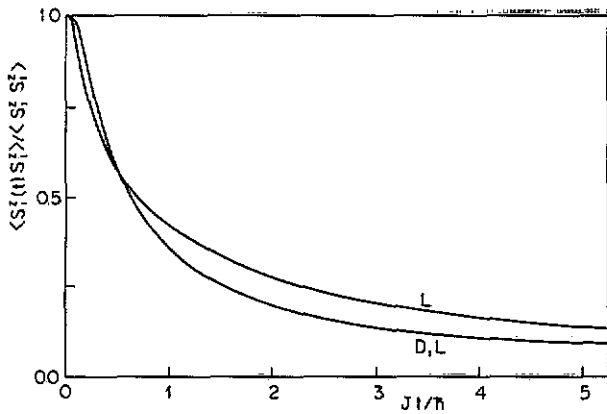

Figure 8. Diffusive spin correlation functions for L and DL systems with the values of D_ν given in the text.

consequent cross with the DL decay. Although in the L-systems the decay is approximately 1D ($m_2(t) \approx 1$) until times of the order of $a_1 a_2 \sqrt{D_1 D_2}$, we can consider, within a good approximation, that the correlation function behaves two dimensionally at times in the range $\hbar/J < t < a_3^2/D_3 \approx 10^3\hbar/J$. Thus, the product of the error functions in equation (11) decays with $(D_{\rm eff}t/a_1a_2)^{-1}$ where $D_{\rm eff} = \sqrt{D_1 D_2}$.

In order to evaluate the linewidth equation (6) we separate the integral in the integration ranges: $[0, \hbar/J]$, $[\hbar/J, 10^3\hbar/J]$ and $[10^3\hbar/J, \infty]$. The integral over the third range may be neglected because, having a 3D decay, it converges very quickly. Also, it can be seen in figure 8 that the integral over the first zone is approximately equal in L and DL systems and it gives a negligible contribution when compared with the second integral. Thus, in order to describe the relationship between the L and DL EPR linewidths we can consider only the integral over the intermediate range $[\hbar/J, 10^3\hbar/J]$. The result is:

$$\Delta B_1(\theta,\phi)_{\rm DL}/\Delta B_1(\theta,\phi)_L \simeq D_{\rm eff}^{\rm L}/D_{\rm eff}^{\rm DL}. \tag{13}$$

Note that the linewidth ratio is determined by the functional expression of τ_ϕ, and it is independent of any constant factor in equation (8). When the result $D_{\rm eff}^{\rm L}/D_{\rm eff}^{\rm DL} \simeq$

0.54 is compared with the value 0.40 ± 0.02 obtained from the experimental data, it shows the consistency of the microscopic model for superexchange, which led us to the relations between the values of J_ν, and the description of the spin dynamics.

5. Discussion

The result obtained using the present model and magnetostructural correlation data reproduces well the differences between the experimental linewidth data on L and DL systems. In contrast, a gaussian decay, $\exp(-\omega_e^2 t^2/2)$, for the spin correlation function as that obtained for the short-time regime, $t < \hbar/\omega_e$, using the Kubo and Tomita formalism, would lead us to predict a faster decay, and consequently a narrower line, for the L compounds. This is because $\omega_e \propto \sqrt{z_1 J_1^2 + z_2 J_2^2 + z_3 J_3^2}$ is larger for the L systems when the arithmetic or the geometric mean of the exchange coupling constants (J_ν) is conserved from the DL to the L systems. Hence, it is clear that the low-dimensional effects cannot be neglected and the theory must be able to follow the details of the exchange network even in the cases where its dimensionality is not one or two but something in between. Our model satisfies this condition, and allows us to determine the classical diffusion constant as a function of the Heisenberg exchange couplings in their whole range of variation. We should mention, however, that this model fails to describe the angular variation of the experimental ratio $\Delta B(\theta,\phi)_{DL}/\Delta B(\theta,\phi)_L$ which can be estimated from figures 5 and 6. This limitation arises from the fact that the model only considers interactions linear in electronic spin operators, while the experimental linewidths also contain contributions from interactions bilinear in electronic spin operators, such as the magnetic dipolar and antisymmetric exchange. These interactions are the source of the angular variation of the experimental ratio because even when the arrangement of coppers is almost identical in the L and DL systems of the same amino acid, the difference in the exchange networks produces different angular variations for the dipolar contribution in each system. This problem has been recently investigated by Calvo *et al* [6b]. They show the different angular variations for the dipolar contribution in square lattices of spin 1/2 resulting on changing the exchange network from 2D to 1D. Besides, we have calculated the time evolution of the angular variation of the correlation functions for the dipolar interaction in the simpler case of a square lattice of spins 1/2 with an isotropic exchange network [22]. From those works, we conclude that even when the model introduced here can be refined to deal with interactions bilinear in electronic spins, this would require a numerical approach involving the evaluation of spin correlation functions of different pairs, which for these systems of low symmetry implies a computational effort beyond the scope of this work.

Using our simple model, it is also possible to explain the difference in linewidth between both DL systems. As can be seen in table 1, the interlayer distance in Cu(DL-BUT)$_2$ is around 5 Å shorter than in Cu(DL-MET)$_2$, leading to a larger exchange coupling J between layers, in the first complex. This produces an earlier cut-off of the zone with 2D decay and consequently a narrower line for Cu(DL-BUT)$_2$ with respect to Cu(DL-MET)$_2$.

Acknowledgments

We are very grateful to Drs A M Gennaro, M C G Passeggi and M Ebersole for valuable discussions. We also acknowledge to Professors H J Schugar and G J Palenik who

supplied us with crystallographic information about Cu(DL-MET)$_2$ and Cu(L-MET)$_2$. The experimental part of this work was supported by grants 3-905608, 3-905604 and 3-098700/88 of the Consejo Nacional de Investigaciones Científicas y Técnicas (CONICET), Argentina, grant RG86-14 of the Third World Academy of Sciences and by Fundación Antorchas, Argentina. HMP received support from the Organization of the American States.

References

[1] Willett R D, Gatteschi D and Kahn O 1984 *Magneto Structural Correlations in Exchange Coupled Systems (NATO ASI Series)* (Dordrecht: Reidel)
[2] Richards P M 1975 *Local Properties at Phase Transitions* (Bologna: Editrice Compositori) p 539
[3a] Gennaro A M, Levstein P R, Steren C A and Calvo R 1987 *Chem. Phys.* **111** 431
[3b] Steren C A, Gennaro A M, Levstein P R and Calvo R 1989 *J. Phys.: Condens. Matter* **1** 637
[4] Levstein P R, Steren C A, Gennaro A M and Calvo R 1988 *Chem. Phys.* **120** 449
[5] Levstein P R and Calvo R 1990 *Inorg. Chem.* **29** 1581
[6a] Calvo R, Novak M, Oseroff S and Symko O G 1987 *Oyo Butsuri* **26** 861
[6b] Calvo R, Passeggi M C G, Novak M, Symko O G, Oseroff S B, Nascimento O R and Terrile M C 1991 *Phys. Rev.* B **43** 1074
[7a] Veidis M V and Palenik G J 1969 *Chem. Commun.* 1277
[7b] Veidis M V 1969 *PhD Thesis* University of Waterloo, Ontario
[8] Ou C C, Powers D A, Thich J A, Felthouse T R, Hendrikson D N, Potenza J A and Schugar H J 1978 *Inorg. Chem.* **17** 34
[9] Fawcett T G, Ushay M, Rose J P, Lalancette R A, Potenza J A, and Schugar H J 1979 *Inorg. Chem.* **18** 327
[10] Levstein P R, Calvo R, Castellano E E, Piro O E and Rivero B E 1990 *Inorg. Chem.* at press
[11] Kubo R and Tomita J 1954 *Phys. Soc. Japan* **9** 888
[12] Calvo R and Passeggi M C G 1990 *J. Phys.: Condens. Matter* **2** 9113
[13] Moriya T 1963 *Magnetism* vol 1, ed G T Rado and H Suhl (New York: Academic)
[14a] Gennaro A M 1988 *PhD Thesis* Universidad Nacional de Rosario, Argentina
[14b] Gennaro A M and Calvo R 1989 *J. Phys.: Condens. Matter* **1** 7061; 1990 *J. Phys.: Condens Matter* **2** 2873
[15a] Blume M and Hubbard J 1970 *Phys. Rev.* B **1** 3815
[15b] Bennett H S and Martin P C 1965 *Phys. Rev.* A **138** 608
[15c] Kadanoff L P and Martin P C 1963 *Ann. Phys.* **24** 419
[16] Newman P R, Imes J L and Cowen J A 1976 *Phys. Rev.* B **13** 4093
[17a] Anderson P W 1958 *Phys. Rev.* 109 1492
[17b] Anderson P W 1978 *Rev. Mod. Phys.* **50** 181
[17c] Anderson P W 1983 *Physica* **117B, 118B** 30
[18a] Thouless D J 1980 *Solid State Commun.* **34** 683
[18b] Pastawski H M unpublished
[19] Montroll E W and West B J 1987 *Fluctuation Phenomena* ed E W Montroll and J L Lebowitz (Amsterdam: Elsevier) p 61
[20a] De Masi A, Ferrari P A and Lebowitz J L 1985 *Phys. Rev. Lett.* 55 1947
[20b] Lebowitz J L 1986 *Physica* **140A** 232
[21] Levstein P R, Pastawski H M, D'Amato J L 1990 *J. Phys.: Condens. Matter* **2** 1781
[22] Gennaro A M and Levstein P R 1991 *J. Phys.: Condens. Matter* **3** 455